PHYSICAL REVIEW C VOLUME 18, NUMBER 4 OCTOBER 1978

Electromagnetic transitions between the low-lying levels of ^{21}Ne and their relation to parity mixing of the 2.80-MeV $1/2^{\pm}$ doublet

D. J. Millener and E. K. Warburton
Brookhaven National Laboratory, Upton, New York 11973

K. A. Snover, R. von Lintig, and P. G. Ikossi
Department of Physics, University of Washington, Seattle, Washington 98195

(Received 8 June 1978)

The presence of a $J^{\pi} = 1/2^{+}$-$1/2^{-}$ doublet ($\Delta E \simeq 8$ keV) at 2.80 MeV in ^{21}Ne provides an opportunity to further investigate parity mixing of nuclear states. The parity mixing in ^{21}Ne introduces an irregular $M1$, $E2$ admixture into the regular, but highly retarded, $E1$, $M2$ decay of the $1/2^{-}$ level to the $3/2^{+}$ ground state and can be inferred from the interference between these irregular and regular decays. We consider the dependence of possible ^{21}Ne parity-mixing observables on the four electromagnetic matrix elements involved in the transition and also methods for determining these matrix elements. The first step towards a measurement of the $M2/E1$ mixing ratio is a measurement of the $E3/M2$ mixing ratio of the $1/2^{-} \rightarrow 5/2^{+}$ transition in ^{21}Ne and this is carried out using a γ-γ correlation utilizing the ^{18}O(α,n) ^{21}Ne reaction. A large basis SU(3) shell-model calculation is performed to give wave functions for ^{21}Ne (and ^{21}Na) and predictions for the electromagnetic matrix elements relevant to studies of the $1/2^{\pm}$ parity mixing. The parity-mixing matrix element is calculated using a one-body approximation to the parity nonconserving interaction. The calculated matrix elements are compared with the available experimental data on ^{21}Ne and ^{21}Na.

[NUCLEAR STRUCTURE ^{21}Ne, ^{21}Na; calculated nuclear wave functions, electromagnetic, parity-mixing matrix elements. SU(3) shell-model method. ^{21}Ne; measured γ-γ $\frac{1}{2}^{-} \rightarrow \frac{5}{2}^{+} \rightarrow \frac{3}{2}^{+}$ angular correlation. Deduced $\frac{1}{2}^{-} \rightarrow \frac{5}{2}^{+}$ $E3/M2$ mixing ratio. ^{21}Ne; calculated γ-ray CP and asymmetry formulas for polarized and unpolarized beams.]

I. INTRODUCTION

The search for parity mixing in nuclear wave functions commenced[1] very soon after the discovery of parity nonconservation in weak interactions,[2,3] and a number of examples of the effects of such mixing have now been observed in α decay[4] (one case, ^{16}O) and in electromagnetic transitions (see Refs. 5 and 6 for a review). From an analysis of these results one hopes to learn more about the detailed form of the weak interaction Hamiltonian. However, the path from the weak-interaction Hamiltonian to parity admixtures in nuclear wave functions is not a direct one. First, a parity-nonconserving (PNC) nucleon-nucleon (NN) interaction must be calculated using meson theory (since the hard-core in the NN interaction strongly reduces the effect of a direct weak interaction). Second, reliable microscopic nuclear wave functions must be available so that the parity mixing may be calculated once a PNC interaction is specified. Since PNC interactions have important short-range components arising from ρ exchange, correlated two-particle wave functions must be used in the calculations, i.e., the Bethe-Goldstone equation or some equivalent must be solved.

Unfortunately, most of the existing measurements on PNC electromagnetic transitions have been made for heavy nuclei where it is most difficult to make sufficiently detailed nuclear structure calculations. In fact, the only positive electromagnetic result amongst the light nuclei (if we exclude the two-nucleon system for which the experimental problems are formidable) is for ^{19}F (Ref. 7). Since the ^{19}F states involved have isospin $T = \frac{1}{2}$ both the isoscalar and the isovector parts of the PNC NN interaction can contribute to the observed parity mixing. It would be very desirable to separate the isoscalar and isovector contributions since neutral weak currents may strongly enhance the $\Delta T = 1$ parity mixing but are not expected to affect the isoscalar term appreciably.[8]

If the effects of the isoscalar and isovector PNC interaction are to be separated another measurement is required. One such measurement[9] on ^{18}F, which is sensitive to only the isovector PNC interaction, provides a limit on the mixing of a 0^{-} $T = 0$ level with a 0^{+} $T = 1$ level. Another possibility is to study another $T_z = \frac{1}{2}$ nucleus where, due to the structure of the levels involved, the mixing is sensitive to a different linear combination of isoscalar and isovector interactions than is the case for ^{19}F. The presence of a $\frac{1}{2}^{+}$ level in ^{21}Ne 8 keV above the 2789-keV $\frac{1}{2}^{-}$ level[10] (see Fig. 1) together with the

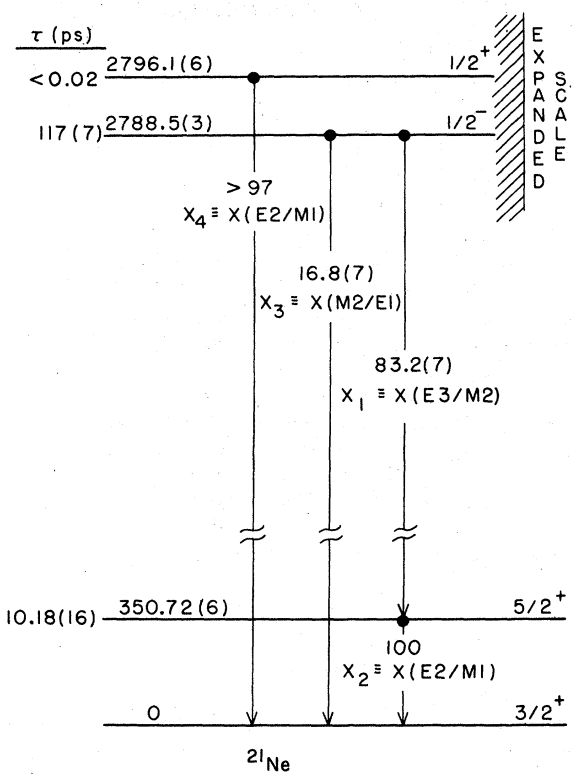

FIG. 1. The ^{21}Ne energy levels and γ-ray transitions pertinent to the present studies. The level energies (in keV), spins, parities, and γ-ray branching ratios (in percent) are from Ref. 10 as is the lifetime limit for the 2796-keV level. The meanlives adopted for the 351- and 2789-keV levels are weighed averages as discussed in the text and summarized in Table II. The four $x(L+1/L)$ mixing ratios are labeled for easy reference.

strong inhibition of the $E1$ $\frac{1}{2}^- \rightarrow \frac{3}{2}^+$ ground-state transition [$\lesssim 9\times 10^{-8}$ Weisskopf units[11] (W.u.)] makes the $\frac{1}{2}^-$ level an attractive candidate for parity-mixing studies to complement the information obtained from the ^{19}F $\frac{1}{2}^- \rightarrow \frac{1}{2}^+$ transition.[12,6]

In this paper we shall be concerned with three topics. First, we wish to display the dependence of possible parity-mixing experiments on the electromagnetic decay properties of the $\frac{1}{2}^\pm$ doublet of ^{21}Ne. Second, we present a measurement of one of these properties—namely, the $E3/M2$ mixing ratio of the 2789 → 351 $\frac{1}{2}^- \rightarrow \frac{5}{2}^+$ transition (see Fig. 1). Third, we present the results of a relatively large-basis shell-model study of the low-lying levels of ^{21}Ne (and their analogs in ^{21}Na) with particular reference to those electromagnetic properties relevant to the present problem.

To illustrate the dependence of one possible ^{21}Ne parity-mixing measurement on the electromagnetic decay properties we note that if the parity-mixed $\frac{1}{2}^-$ level is produced polarized in a nuclear reaction the angular distribution of γ rays for the ground-state transition will not in general be isotropic [Eq. (19)]. The coefficient (A_γ) of $\cos\theta$ in the angular distribution is a measure of the parity admixture and the expression for A_γ involves the quadrupole/dipole mixing ratios of the $\frac{1}{2}^- \rightarrow \frac{3}{2}^+$ and $\frac{1}{2}^+ \rightarrow \frac{3}{2}^+$ transitions [see Fig. 1 and Eq. (15)]. Thus experiments are necessary to determine the relevant mixing ratios and transition rates. Indeed A_γ could conceivably vanish due to $E1$-$M2$ interference effects independent of the parity mixing in the $\frac{1}{2}^-$ wave function. Although the important $M2/E1$ mixing ratio for the $\frac{1}{2}^- \rightarrow \frac{3}{2}^+$ transition cannot be measured easily, it *can* be measured by comparing the circular polarizations of the $\frac{1}{2}^- \rightarrow \frac{3}{2}^+$ and $\frac{1}{2}^- \rightarrow \frac{5}{2}^+$ transitions following formation via a polarized beam, provided the $E3/M2$ mixing ratio for the latter transition is known. As described in Sec. III, this $E3/M2$ mixing ratio may be obtained from the directional correlation between the γ rays in the $\frac{1}{2}^- \rightarrow \frac{5}{2}^+ \rightarrow \frac{3}{2}^+$ cascade and the measured $E2/M1$ mixing ratio of the $\frac{5}{2}^+ \rightarrow \frac{3}{2}^+$ transition. A more general reason for measuring the $E3/M2$ mixing ratio of the $\frac{1}{2}^- \rightarrow \frac{5}{2}^+$ transition is that the circular polarization of this transition is expected to provide the best measurement of the polarization of the $\frac{1}{2}^-$ state and the mixing ratio is needed to make this calibration quantitative in any measurements using a polarized beam.

All the formulas relevant to the experimental measurement of the mixing ratios and the parity mixing effects are given in Sec. II. The experimental measurement of the $E3/M2$ mixing ratio for the $\frac{1}{2}^- \rightarrow \frac{5}{2}^+$ transition, the first step in the series of experiments proposed above, is presented in Sec. III. Section IV is devoted to the mass 21 shell-model study and a comparison of these calculations with the available experimental data including the present measurement. Finally, Sec. V contains a summary and discussion.

II. RELEVANT FORMULAS

It is, of course, important to insure phase consistency in the definitions of mixing ratios appearing in the different experiments and in the comparison of these experiments with model calculations. Therefore, the γ-γ correlation, circular polarization, and asymmetry formulas presented here were all calculated from the same general relationship; namely, Eq. (3.32) of Rose and Brink.[13] The γ-ray transitions of interest here are all indicated in Fig. 1.

γ-γ directional correlation. The directional correlation, $W(\theta)$, between γ_1 and γ_2 in the cascade $\frac{1}{2}^- \xrightarrow{\gamma_1} \frac{5}{2}^+ \xrightarrow{\gamma_2} \frac{3}{2}^+$ is written as

$$W(\theta) = A_0[1 + a_2 P_2(\cos\theta) + a_4 P_4(\cos\theta)], \quad (1)$$

where A_0 is an arbitrary normalization and θ is the angle between the directions of emission of γ_1 and γ_2. In the present case it is convenient to write a_2 and a_4 in the form

$$a_k = -0.2000 Q_k^{(1)} Q_k^{(2)} f_k(x_1) f_k(x_2), \quad (2)$$

where the $Q_k^{(i)}$ are the usual solid angle attenuation coefficients for $\gamma_1 (i=1)$ and $\gamma_2 (i=2)$, and the $f_k(x_i)$ are functions of the mixing ratios of the two transitions: $x_1 \equiv x(E3/M2)$ and $x_2 \equiv x(E2/M1)$. The functions f_k are given by

$$f_2(x_1) = (1 + 1.4142x_1 + 1.5000x_1^2)/(1 + x_1^2), \quad (3a)$$

$$f_2(x_2) = (1 + 5.0709x_2 - 0.5102x_2^2)/(1 + x_2^2), \quad (3b)$$

$$f_4(x_1) = (1 - 3.5355x_1 - 0.2500x_1^2)/(1 + x_1^2), \quad (4a)$$

$$f_4(x_2) = 2.1769x_2^2/(1 + x_2^2). \quad (4b)$$

The mixing ratio of the 351-keV $\frac{5}{2}^+ \rightarrow \frac{3}{2}^+$ transition can be obtained with relatively high precision by combining Coulomb excitation measurements of the $B(E2)$ value with mean life τ measurements of the 351-keV level:

$$\tau/\tau(E2) = x_2^2/(1 + x_2^2), \quad (5a)$$

where

$$\tau(E2) = 816.1 E_\gamma^{-5}/B(E2), \quad (5b)$$

with τ in ps, E_γ in MeV, and $B(E2)$ in $e^2\text{fm}^4$.

The $B(E2)$ value of the $\frac{5}{2}^+ \rightarrow \frac{3}{2}^+$ transition has recently been measured as 71 ± 10 e^2 fm^4 and 93 ± 13 e^2 fm^4 from Coulomb excitation of ^{21}Ne by ^{32}S (Ref. 14) and protons (Ref. 15) respectively. We adopt 82 ± 11 e^2 fm^4 as the best value of $B(E2)$ from these two measurements.

For τ we take the weighed average of the most recent five measurements quoted by Rowe *et al.*[16] The pre-1975 measurements are not considered reliable enough for inclusion. The result is 10.18 ± 0.16 ps, in excellent agreement with the most accurate two measurements—both obtained via the recoil distance method—of 10.1 ± 0.3 ps (Ref. 17) and 10.23 ± 0.20 ps (Ref. 16).

From Eq. (5) we then have

$$x_2 = +0.0739 \pm 0.0048, \quad (6)$$

where we have used $E_\gamma = 350.72 \pm 0.006$ keV (Ref. 18) and the plus sign for x_2 is taken from the results of Pronko *et al.*[19] In addition, as will be shown in Sec. III, the present γ-γ correlation results eliminate the minus sign alternative. Inserting the value of x_2 from Eq. (6) into Eqs. (3b) and (4b), we have, from Eq. (2),

$$a_2 = -(0.2717 \pm 0.0046) Q_2^{(1)} Q_2^{(2)} f_2(x_1) \quad (7a)$$

and

$$a_4 = -(0.0024 \pm 0.0003) Q_4^{(1)} Q_4^{(2)} f_4(x_1). \quad (7b)$$

γ-ray circular polarization with a polarized initial state. If the ^{21}Ne $\frac{1}{2}^-$ state is polarized by formation via a nuclear reaction initiated by a polarized beam then, in general, the γ rays corresponding to the $\frac{1}{2}^- \rightarrow \frac{3}{2}^+$ and $\frac{1}{2}^- \rightarrow \frac{5}{2}^+$ transitions will be circularly polarized.

With $P^q(k)$ defined[13] as the probability per unit time and unit solid angle that the nucleus emits a γ ray in the direction k with polarization q, the fractional degree of γ-ray circular polarization is defined as

$$P_\gamma = (P^1 - P^{-1})/(P^1 + P^{-1}) \quad (8)$$

where $q = +1$ and -1, for right- and left-handed circular polarization, respectively. Similarly, the polarization magnitude $P_W(J_1)$ of the $J_1 = \frac{1}{2}$ initial state is defined as

$$P_W(\tfrac{1}{2}) = [W(\tfrac{1}{2}) - W(-\tfrac{1}{2})]/[W(\tfrac{1}{2}) + W(-\tfrac{1}{2})], \quad (9)$$

where $W(m)$ is the relative population of the mth substate along the axis of quantization, which is chosen in the direction of polarization $\hat{e}_q$. With these definitions, and assuming parity conservation, the degree of γ-ray circular polarization, $P(J_1, J_2)$, for the $\frac{1}{2}^- \rightarrow J_2$ transition is related to the polarization of the initial $(J_1 = \frac{1}{2})$ state by

$$P_\gamma(\tfrac{1}{2}, J_2) = P_W(\tfrac{1}{2}) f_1(\tfrac{1}{2}, J_2) P_1(\cos\theta), \quad (10)$$

where $\cos\theta = \hat{e}_q \cdot \vec{k}/k$.

For the $\frac{1}{2}^- \rightarrow \frac{5}{2}^+$ and $\frac{1}{2}^- \rightarrow \frac{3}{2}^+$ transitions we have

$$f_1(\tfrac{1}{2}, \tfrac{5}{2}) = -0.3333(1 - 5.6569x_1 - x_1^2)/(1 + x_1^2), \quad (11a)$$

where $x_1 \equiv x(E3/M2)$ and

$$f_1(\tfrac{1}{2}, \tfrac{3}{2}) = -0.5000(1 - 3.4641x_3 - x_3^2)/(1 + x_3^2), \quad (11b)$$

where $x_3 \equiv x(M2/E1)$. With x_1 obtained from a γ-γ correlation measurement via Eq. (7), the most straightforward method of measuring x_3 would appear to be from the ratio $P_\gamma(\frac{1}{2}, \frac{3}{2})/P_\gamma(\frac{1}{2}, \frac{5}{2})$ which from Eq. (10) is just $f_1(\frac{1}{2}, \frac{3}{2})/f_1(\frac{1}{2}, \frac{5}{2})$.

γ-ray circular polarization from an unpolarized initial state. If the $\frac{1}{2}^-$ initial state is unpolarized then any γ-ray circular polarization must arise from parity admixtures in the initial or final states. Assuming, in the present case, that the only significant parity admixture arises from interaction of the $\frac{1}{2}^+$ doublet at 2.80 MeV in ^{21}Ne, the circular polarization of the $\frac{1}{2}^- \rightarrow \frac{3}{2}^+$ transition is given by

$$P'_\gamma(\tfrac{1}{2}, \tfrac{3}{2}) = 2\epsilon_1 f'_0(\tfrac{1}{2}, \tfrac{3}{2}), \quad (12)$$

where the primes denote an unpolarized initial state and parity nonconservation. $\epsilon_1 \equiv x(M1/E1)$

gives a direct measure of the parity admixture. The function $f_0'(\frac{1}{2}, \frac{3}{2})$ contains the dependence of the circular polarization on the quadrupole admixtures in the $\frac{1}{2}^- \rightarrow \frac{3}{2}^+$ and $\frac{1}{2}^+ \rightarrow \frac{3}{2}^+$ transitions, i.e.,

$$f_0'(\tfrac{1}{2}, \tfrac{3}{2}) = (1 + x_3 x_4)/[1 + x_3^2 + \epsilon_1^2(1+x_4^2)], \qquad (13)$$

where $x_3 \equiv x(M2/E1)$ and $x_4 \equiv x(E2/M1)$ are indicated in Fig. 1.

γ-ray asymmetry from a polarized initial state. If the $\frac{1}{2}^-$ initial state is polarized by formation via a nuclear reaction initiated by a polarized beam then the angular distribution of the $\frac{1}{2}^- \rightarrow \frac{3}{2}^+$ transition relative to the polarization direction $\hat{e}_z$ also provides a measure of the parity admixture via $\epsilon_1 \equiv x(M1/E1)$:

$$W(\theta) = 1 + A_\gamma P_1(\cos\theta) = 1 - P_W(\tfrac{1}{2})\epsilon_1 f_1'(\tfrac{1}{2}, \tfrac{3}{2}) P_1(\cos\theta), \qquad (14)$$

where A_γ is the asymmetry, $P_W(\frac{1}{2})$ is given by Eq. (9), and

$$f_1'(\tfrac{1}{2}, \tfrac{3}{2}) = \frac{[1 - 1.7321(x_3 + x_4) - x_3 x_4]}{1 + x_3^2 + \epsilon_1^2(1 + x_4^2)}. \qquad (15)$$

III. EXPERIMENTAL RESULTS FOR THE $E3/M2$ MIXING RATIO OF THE $1/2^- \rightarrow 5/2^+$ TRANSITION

Here we describe the results of angular correlation measurements for the $\frac{1}{2}^- \xrightarrow{\gamma_1} \frac{5}{2}^+ \xrightarrow{\gamma_2} \frac{3}{2}^+$ γ-γ cascade ($E_{\gamma_1} = 2.44$ MeV and $E_{\gamma_2} = 0.35$ MeV). The $\frac{1}{2}^-$ level was populated in the $^{18}O(\alpha, n)$ ^{21}Ne reaction [$Q_0 = -696$ keV (Ref. 10)] at $E_\alpha = 5.10$ MeV. This α energy corresponds to a maximum excitation energy of 3.47 MeV in ^{21}Ne, so that the only levels above the $\frac{1}{2}^-$ which were populated were the $\frac{1}{2}^+$, 2796-keV and $\frac{9}{2}^+$, 2866-keV levels.[10] A 70-nA α^+ beam was produced by the University of Washington FN tandem Van de Graaff and stopped in a tantalum target of thickness 0.012 cm, with an oxidized ^{18}O surface layer of ^{18}O areal density ~220 $\mu g/cm^2$. A 4.45-cm-diam by 5.08-cm-long cylindrical NaI crystal mounted on an RCA 8575 phototube was used to detect the 351-keV γ rays, and an ORTEC coaxial Ge(Li) detector of 15% efficiency (relative to a 7.5 × 7.5-cm NaI detector) was used to detect γ rays between energies of 0.75 and 3.0 MeV. The front face of the NaI detector was located 8.3 cm from the target, while that of the Ge(Li) detector was at 8.9 cm. The NaI detector was fixed at an angle of −135° with respect to the beam axis, and the Ge(Li) detector—coplanar with the beam axis and the NaI detector—was set at angles of 45°, 15°, −15°, and −45° to the beam axis, corresponding to the relative γ-γ correlation angles $\theta = 180°$, 150°, 120°, and 90°. This arrangement insured that the Ge(Li) detector would view the same beam-related background (and the same Doppler-related effects) for $\theta = 180°$ and 90°—the most important correlation angles.

Signals corresponding to fast coincidences between the two detectors were produced in a time-to-amplitude converter (TAC) using leading edge timing for the short rise time NaI signals and extrapolated zero strobe timing for the Ge(Li) signals. Three-parameter coincidence events (parameters E_γ(NaI), E_γ[Ge(Li)], and TAC amplitude) were recorded in a computer, along with Ge(Li) singles recorded in a separate analyzer. A gain stabilizer centered on the 351-keV γ ray was used with the NaI detector.

Coincidence data analysis was performed in two stages. First, NaI spectra were generated corresponding to windows set on the 2.44-MeV peak in the Ge(Li) spectrum and on the TAC peak; an example is shown in Fig. 2. These spectra are dominated by the 351-keV line, with no evidence for other significant contributions. Centroids calculated from these spectra were used to compute small residual gain correction factors (which were ~±0.3%) which were applied to the results discussed below. Second, Ge(Li) difference spectra were generated corresponding to a window centered on the 351-keV line in the NaI spectrum and (reals plus random) minus (random) TAC windows (the random correction was ~3%)—an example is shown in Fig. 3 (lower). A substantial reals continuum background is apparent in this spectrum, along with some apparent reals contribution from the 2.8 → 0 γ decays presumably arising from n-γ coinciden-

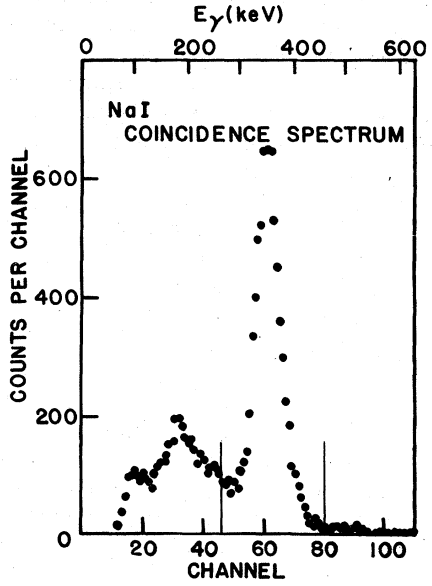

FIG. 2. NaI coincidence spectrum generated from a TAC reals window and an energy window centered on the 2.44-MeV Ge(Li) peak. The NaI energy window used in subsequent analysis is indicated by vertical lines.

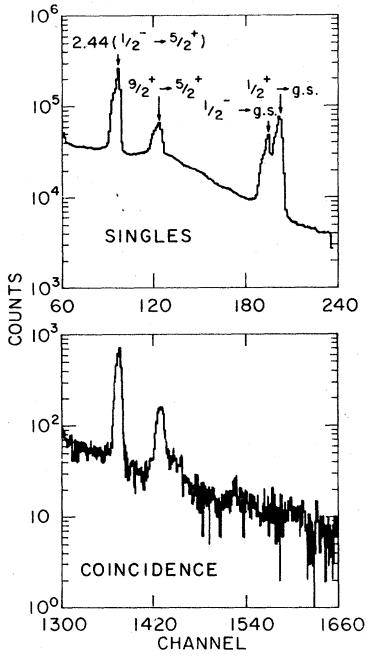

FIG. 3. Coincidence (lower) and singles (upper) Ge(Li) γ-ray spectra for $2.2 < E_\gamma < 3.0$ MeV at $\theta = 150°$ ($\theta_{beam} = 15°$) from the $^{18}O(\alpha, n\gamma)^{21}Ne$ reaction at $E_\gamma = 5.1$ MeV.

ces in which the neutron was detected in the NaI detector. Coincidence yields for the $2.80 \rightarrow 0.35 \rightarrow 0$ cascade were then extracted from these spectra by summing counts above a symmetric background determined from regions above and below the centroid of the 2.44-MeV Ge(Li) peak.

Care was taken in the choice of background windows here and in the singles analysis to minimize the effect of a possible $\frac{1}{2}^+ \rightarrow \frac{5}{2}^+$ branch. There is no evidence from the present data for such a branch. A proper accounting of the uncertainty in background shape in the region where such a peak is expected leads us to an upper limit of 3% for this decay relative to the $\frac{1}{2}^+ \rightarrow \frac{3}{2}^+$ decay. This limit is similar to that obtained previously.[10]

The Ge(Li) singles spectra [see Fig. 3 (upper)] were analyzed with a similar background subtraction to determine the intensities of the γ-ray peaks at 2.44 and 2.80 MeV; the latter containing the ground-state transitions of both the $\frac{1}{2}^+$ and $\frac{1}{2}^-$ levels. Since these peaks arise from decays of $J = \frac{1}{2}$ initial states, the angular distributions of their intensities should be isotropic. However, small systematic variations as a function of angle and fluctuating variations independent of angle were present in these yields when normalized to total integrated beam current. These variations could arise from a small geometrical misalignment, and an inaccuracy in beam-current integration, respectively.

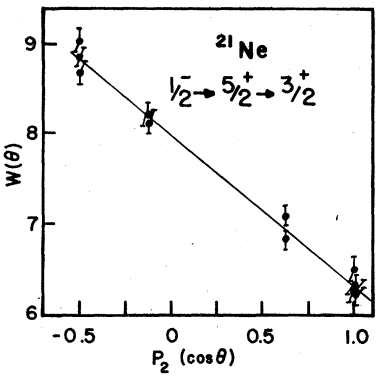

FIG. 4. Results for the ^{21}Ne $\frac{1}{2}^- \rightarrow \frac{5}{2}^+ \rightarrow \frac{3}{2}^+$ relative γ-γ correlation $W(\theta)$ of Eq. (1) versus $P_2(\cos\theta)$. The solid line is the best fit allowing only A_0 and a_2 to vary ($a_4 \equiv 0$) and is indistinguishable from a fit in which a_4 was also free to vary.

Since such variations should affect equally the singles and coincidence yields, our best values for the normalized relative coincidence yield $W(\theta)$ are given by the ratio of measured coincidence counts to 2.44-MeV singles counts. This ratio, which includes small ($\lesssim 1\%$) relative dead time corrections, is plotted against $P_2(\cos\theta)$ in Fig. 4.

A fit to all the data points in Fig. 4 yields $a_2 = -0.2127 \pm 0.0088$ and $a_4 = +0.004 \pm 0.011$, with $\chi^2 = 1.3$. A fit with a_4 constrained to be zero [see Eq. (7)] produces the straight line shown in Fig. 4, with $a_2 = -0.2106 \pm 0.0065$ and $\chi^2 = 1.2$. A fit excluding the 120° and 150° data gives essentially the same a_2.

Various other analyses were performed to investigate effects of systematic errors in the analysis. Different types of coincidence background subtraction were performed; normalizations were also calculated relative to the 2.80-MeV singles yields, which were found to be less sensitive to background subtraction than the 2.44-MeV singles yields. From fits to all of these results with a_4 constrained to be zero we arrive at a best value of $a_2 = -0.2130 \pm 0.0076$, where the above error contains a contribution of ± 0.004 folded with the statistical error to represent the variation observed from the different analyses. Fits in which a_4 was allowed to vary produced values which ranged over $\pm 1\sigma$ ($\sigma = 0.011$) for the different analyses; hence our best value is $a_4 = 0.00 \pm 0.015$. The χ^2 for all of these fits were ≤ 1.3. Attenuation coefficients were calculated from the known geometry of the detectors; the result is $Q_2(\text{NaI})Q_2(\text{GeLi}) = 0.931$ and $Q_4(\text{NaI})Q_4(\text{GeLi}) = 0.79$. Hence from Eq. (7a) we find $f_2(x_1) = +0.842 \pm 0.033$ and $x_1 = -0.12 \pm 0.03$ based on the measured a_2 (this result supersedes an earlier preliminary value[20]). The other solution is $x_1 = -2.03 \pm 0.14$ which is ruled out since it would correspond

to an $E3$ strength of ~870 W.u.; a value which exceeds the recommended upper limit[21] of 100 W.u. The expected a_4 based on the above x_1 and Eq. (7b) is well within the experimental uncertainty of the measured value. Our value for x_1 is in agreement with an earlier, less accurate result[22] of $x_1 = -0.02 \pm 0.14$ (the corrected uncertainty quoted here is based on the measured a_2 quoted in Ref. 22).

Although the sign of x_2, the $0.35 \to 0$ $E2/M1$ mixing ratio, was fairly well determined as even by Pronko *et al.*,[19] it is useful to note that the above a_2 also rules out the opposite (odd) sign, since the minimum x_1 solution for $x_2 = -0.0739 \pm 0.0048$ corresponds to an unreasonably large[21] $E3$ strength of 350 ± 100 W.u. in the $\frac{1}{2}^- \to \frac{5}{2}^+$ transition.

IV. SHELL MODEL STUDY

A. Introduction

The $\frac{1}{2}^- \to \frac{3}{2}^+$ transition is of interest for either of the two possible parity mixing experiments discussed above. We write the initial and final wave functions as (see the level scheme in Fig. 1)

$$\psi_i = \psi(\tfrac{1}{2}^-) - \Delta E^{-1} \langle \tfrac{1}{2}^+ | V_{\mathrm{PNC}} | \tfrac{1}{2}^- \rangle \psi(\tfrac{1}{2}^+), \qquad (16)$$

$$\psi_f = \psi(\tfrac{3}{2}^+),$$

where $\Delta E = 7.6 \pm 0.7$ keV (Ref. 10) and V_{PNC} is the PNC interaction. The wave functions on the right-hand side are taken to be eigenfunctions of the dominant parity conserving part of the Hamiltonian which, for our purposes, is the shell model Hamiltonian. Since ΔE is very small it may be safely assumed that the only significant parity mixing is between the $\frac{1}{2}^+$ and $\frac{1}{2}^-$ levels.

The experimentally observable quantities which give a measure of the parity admixture are the circular polarization (P_γ') of Eq. (12) and the asymmetry (A_γ) of Eq. (14). Both of these are proportional to the $E1/M1$ mixing ratio, ϵ_1, in the $\frac{1}{2}^- \to \frac{3}{2}^+$ transition. Using Eq. (16), ϵ_1 may be expressed as

$$\epsilon_1 = -\frac{\langle \frac{1}{2}^+ \| M1 \| \frac{3}{2}^+ \rangle \langle \frac{1}{2}^+ | V_{\mathrm{PNC}} | \frac{1}{2}^- \rangle}{\langle \frac{1}{2}^- \| E1 \| \frac{3}{2}^+ \rangle \Delta E}, \qquad (17)$$

where the initial wave functions in the electromagnetic matrix elements are written on the left to emphasize our adherence to the conventions of Rose and Brink,[13] i.e., the electromagnetic matrix elements are given by $[4k/(2L+1)]^{1/2} \langle J_i \| T_L^{(\gamma)} \| J_f \rangle$ with $T_{LM}^{(\gamma)}$ defined in Eq. (3.20) of Ref. 13.

The structure of the isoscalar, isovector, and isotensor PNC interactions comes from using the standard nonrelativistic approximations to obtain a one-meson-exchange PNC interaction. However, the strength of each isospin component depends on the weak interaction model. In particular, neutral currents may strongly enhance the strength of the isovector PNC interaction over its strength in the standard Cabibbo model. The main purpose of parity-mixing experiments in nuclei is to use the experimental data together with nuclear structure calculations to obtain information on the isospin character of V_{PNC}. To extract the parity-mixing matrix element from an experimental measurement of the circular polarization or the asymmetry we need to know the $E1$ and $M1$ matrix elements and to some extent both the signs and magnitudes of the $M2/E1$ and $E2/M1$ mixing ratios in the $\frac{1}{2}^- \to \frac{3}{2}^+$ and $\frac{1}{2}^+ \to \frac{3}{2}^+$ transitions. The $E2/M1$ mixing ratio (x_4) is predicted to be, and surely is, small whereas the $M2/E1$ mixing ratio (x_3) could be large. Under these circumstances A_γ may depend sensitively through f_1' [Eqs. (14) and (15)] on the sign and magnitude of x_3. In fact there is a critical value of x_3 near $+0.58$ for which A_γ vanishes regardless of the amount of parity mixing.

On the other hand, Eq. (13) shows that since x_4 is small the extraction of the magnitude of the parity-mixing matrix element from a circular polarization measurement is much less sensitive to our knowledge of the mixing ratios. The magnitude of the $M1$ matrix element may be directly determined from the lifetime of the $\frac{1}{2}^+$ level whilst, in contrast, x_3^2 may significantly influence the extraction of the $E1$ matrix element.

The signs of the dipole matrix elements only have meaning within the context of our nuclear model. Since the $M1$ transition is predicted to be quite strong the sign may be reliably calculated. On the other hand, the $E1$ matrix element is so weak that its calculated sign cannot be trusted. Instead, to obtain the sign of the $E1$ matrix element, the sign of x_3 from an experimental measurement must be combined with the sign of the theoretical $M2$ matrix element. This estimate may still not be very reliable since in our model there is a cancellation between the isoscalar and isovector contributions to the $M2$ matrix element which results in a rather small matrix element. However, it is the only estimate we can make. Since it is important to know the sign of the parity-mixing matrix element for comparison to weak interaction theories it is necessary, whichever parity-mixing experiment is attempted, to measure x_3 to help fix the sign of the $E1$ matrix element.

We next discuss in general terms the structure of the four levels shown in Fig. 1. We describe our shell-model calculations and compare our predictions for the electromagnetic properties of the four levels with the available experimental data including the present measurement. The evaluation of the parity-mixing matrix element using the two body PNC interaction is beyond the scope of our present shell-model code. However, we do use the

one body approximation to the PNC interaction to demonstrate the sensitivity of the parity-mixing matrix element to the structure of the $\frac{1}{2}^-$ level. This sensitivity is important since the ultimate objective of the studies described in this paper is to help isolate the strengths of the isoscalar and isovector PNC interactions.

B. Positive parity states

The full $(sd)^5$ basis is used in the shell-model calculation. There is a choice amongst a number of different effective interactions, e.g., Kuo-Brown[23] (KB), Kuo,[24] Preedom-Wildenthal[25] (PW), Chung-Wildenthal[26] (CW), etc. Since they all give similar wave functions for the lowest $\frac{3}{2}^+$, $\frac{5}{2}^+$, and $\frac{1}{2}^+$ levels our results will not depend strongly on the particular choice of the *sd* shell interaction. (The interactions differ mainly in the predicted excitation energy of the $\frac{1}{2}^+$ bandhead. The KB interaction puts it lowest at 1.5 MeV and the CW interaction, which includes the $\frac{1}{2}^+$ level in a fit to energy level data, highest at 2.7 MeV.) For consistency we quote our results for the KB interaction since this interaction is used in the calculation of the negative parity wave functions.

In the Nilsson model the $\frac{3}{2}^+$ and $\frac{5}{2}^+$ states are described as members of a band built on an intrinsic state with four particles filling the No. 6 orbit (with asymptotic quantum numbers $[220]\frac{1}{2}^+$) and one particle in the No. 7 orbit ($[211]\frac{3}{2}^+$).[27] In the asymptotic limit such states correspond to pure shell-model basis states with [41] supermultiplet symmetry, (81) SU(3) symmetry and $K_J=\frac{3}{2}$. For a typical deformation and spin orbit strength the single particle orbits are not asymptotic. The tables of Chi[28] show that the orbits involved contain about 93% of the asymptotic orbit at a deformation of $\delta=+0.3$. We therefore expect the shell-model wave functions for the ground-state band members to contain approximately 70% of the (81) representation. This is evident from Table I, as is the clear band relationship of the $\frac{3}{2}^+$ and $\frac{5}{2}^+$ states. Furthermore, as demonstrated by Draayer (Table I of Ref. 29), the (81) components correspond to an essentially pure $K_J=\frac{3}{2}$ structure.

The $\frac{1}{2}^+$ level has been interpreted as a bandhead in which the odd nucleon is promoted from the No. 7 orbit to the No. 9 orbit ($[211]\frac{1}{2}^+$); see the discussion in Ref. 30. This is a natural interpretation to make based on the Nilsson diagram and in the asymptotic limit such a state corresponds to a shell-model state with [41](81) $K_J=\frac{1}{2}$ quantum numbers. However, in the shell-model calculations this configuration dominates the *second* $\frac{1}{2}^+$ state for all effective interactions. As can be seen from Table I the principal component of the $\frac{1}{2}_1^+$ state has [41](62) $K_J=\frac{1}{2}$ quantum numbers. The structure of the (62) intrinsic state in terms of asymptotic Nilsson orbits is 75% (No. 6)^4 No. 11, the remainder being equally (No. 6)^3 (No. 7)^2, (No. 6)^3 (No. 9)^2, and (No. 6)^3 No. 7 No. 9. This structure makes for a natural explanation of the strong excitation of the $\frac{1}{2}^+$ level in the ^{20}Ne$(d,p)^{21}$Ne reaction[31] and the large shift of the $\frac{1}{2}_1^+$ analog levels in ^{21}Ne and ^{21}Na since the No. 11 orbit ($[200]\frac{1}{2}^+$) is asymptotically 67% $s_{1/2}$ (58% for $\delta=+0.3$). In fact the (d,p) spectroscopic factor is well reproduced by the full shell-model calculation.[32] On the other hand, an interpretation in terms of the No. 9 orbit requires an unusually small deformation to explain the data. It is not difficult to understand why the $(81)\frac{1}{2}^+$ state has a moderately high excitation energy (~5.8 MeV for the CW interaction); the state must have orbital angular momentum $L=1$ and as such it cannot have a parentage to the dominant $L=0$ component of the ^{20}Ne ground state.

C. Negative parity states

The calculations for the negative parity states are part of a series of calculations[33] made for negative parity states in the nuclei $A=18-21$. The bases include $1\hbar\omega$ configurations of the type p^{-1}

TABLE I. Summary of wave functions (% intensities).

[f]	(λμ)	$\frac{3}{2}^+$	$\frac{5}{2}^+$	$\frac{1}{2}^+$	(λμ)	$\frac{1}{2}^-$ Small basis	$\frac{1}{2}^-$ Large basis
[41]	(81)	74.05	67.86	12.41	(83)	50.96	42.58
	(62)	7.50	10.85	61.67	(91)	31.63	31.42
	(43)	1.89	2.25	0.00	(64)	4.91	5.02
	(51)	2.18	2.03	0.15	(45)	3.55	4.38
	(24)	0.86	2.37	12.19	(72)	8.48	9.62
[32)	(62)	7.06	6.59	2.43	(11,0)	0.48	0.26
	(43)	0.74	0.67	3.50	(53)		4.46
[311]	(70)	3.20	2.97	0.17	(80)		2.26
	(43)	0.36	0.42	3.74			
Total		97.17	96.01	96.26		100	100

$(sd)^n$ and $(sd)^{n-2}(pf)$. For $A=18$ the complete $1\hbar\omega$ basis is used but for $A=19-21$ truncations are made according to SU(3) symmetry. The interactions used are the KB interaction for the sd shell matrix elements, the Millener-Kurath[34] (MK) interaction for the particle-hole matrix elements and the Kuo bare G matrix for the remaining matrix elements which involve the pf shell orbits. The $A=21$ nuclei provide an important reference point in calculations for negative parity states at the beginning of the sd shell. This is because the $\frac{3}{2}^-_2$ (4.73 MeV) and $\frac{1}{2}^-_2$ (5.69 MeV) levels in ^{21}Ne are thought to have a rather pure $(sd)^4(pf)$ structure based on the No. 14 Nilsson orbit ($[330]\frac{1}{2}^-$). Thus the energies of these levels help to determine the pf single particle energies to be used in the calculations. When the single particle energies are chosen in this way levels in $A=19$ and $A=20$ which are expected to have appreciable pf components are well described by the model.

The SU(3) representations included in the basis for $A=21$ are listed in Table I together with the percentage intensities of each in the $\frac{1}{2}^-_1$ wave function. Actually, wave functions for two calculations, which we refer to as small and large basis calculations, are given. All possible SU(3) representations for $(sd)^6$ and $(sd)^4$ which can couple to a p shell hole or a pf shell particle to form an SU(3) representation in the list of overall SU(3) symmetries are included. The most important configurations for the lowest eigenstates are

$$p^{-1}(01)\times(sd)^6[42](82)\rightarrow(83)(91),$$

$$p^{-1}(01)\times(sd)^6[411](90)\rightarrow(91),$$

and

$$(sd)^4[4](80)\times pf(30)\rightarrow(11,0)(91). \tag{18}$$

A number of spurious (91), (72), (80), and (53) states are eliminated from the basis before diagonalization. Configurations with total intrinsic spin $S\geq\frac{5}{2}$ are omitted, a restriction which eliminates only some states of low spatial symmetry. The resulting matrices for $J=\frac{1}{2}$ and $J=\frac{3}{2}$ in the small basis calculation are of dimension ~100 and ~200, respectively.

When states with (80) and (53) symmetries are added to the $J=\frac{1}{2}$ basis the total number of states rises to ~250 with 80% of the increase coming from states with (53) symmetry. Out of these ~250 states only 15 and 6 occur with intensities $\geq 1\%$ in the $\frac{1}{2}^-_1$, and $\frac{1}{2}^-_2$ wave functions, respectively. Indeed a few states with (83) and (91) symmetry dominate the $\frac{1}{2}^-_1$ wave function whilst the single $(sd)^4(pf)$ (11, 0) state accounts for ~71% of the $\frac{1}{2}^-_2$ wave function. The intensity of pf configurations in the $\frac{1}{2}^-_1$ wave function is small and varies between $1\frac{1}{2}\%$ and 2% depending on the size of the basis and the precise values chosen for the pf single particle energies. About 80% (20%) of the $\frac{1}{2}^-_1$ wave function consists of a hole coupled to six sd shell particles coupled to $T=1(0)$; this is to be compared with the simplest model (see, e.g., Ref. 35) of a $p_{1/2}$ hole coupled to the lowest 0^+ $T=1$ state of $A=22$.

We must ask how adequate our truncation of the basis is for the uses to which we wish to put the $\frac{1}{2}^-$ wave function. We wish to calculate $E1$, $M2$, and $E3$ strengths for transitions to the positive parity levels. The $E1$ operator and the spin part of the $M2$ operator transform as (10) + (01) SU(3) tensors; the $E3$ and the orbital part of the $M2$ operator transform as (21) + (12) SU(3) tensors. Thus the $E1$ operator can connect the dominant (81) component of the $\frac{3}{2}^+$ and $\frac{5}{2}^+$ wave functions to those $1\hbar\omega$ representations which occur in the product

$$(81)\times(10)\rightarrow(91)(72)(80). \tag{19a}$$

Similarly for the dominant (62) component of the $\frac{1}{2}^+$ wave function

$$(62)\times(10)\rightarrow(72)(53)(61). \tag{19b}$$

Hence it is desirable to include all states belonging to representations appearing in Eq. (19) in the negative parity basis, even if the admixtures are small, as they generally will be, since it is just such small admixtures which contribute the bulk of the $E1$ matrix elements. In the case of the large basis calculation only states from the (61) representation have been omitted from the basis. Whilst it is possible to expand the basis further the effect of adding additional representations could certainly be studied in perturbation theory. In fact since the vast majority of states in the large basis calculation contribute minute fractions of a percent to the wave function they could also be treated in perturbation theory; e.g., although inclusion of the (53) representation doubles the size of the basis only two states contribute as much as 1% to the wave function.

An advantage of the SU(3) basis is that it can be systematically expanded to meet requirements such as the one suggested above for $E1$ operators. At each stage spurious center-of-mass states can be eliminated exactly. Another advantage is that all the orbits of a major shell are treated on an equal footing, e.g., in evaluating the matrix elements of spin dependent operators it is important to include both partners of a spin orbit doublet in the basis.

D. Electromagnetic matrix elements

We use oscillator wave functions with the size parameter b fixed at 1.784 fm to calculate the

TABLE II. Comparision of the shell–model predictions to experiment for electromagnetic transitions in ^{21}Ne and ^{21}Na.

Transition $J_i^\pi \to J_f^\pi$	Quantity [a]	^{21}Ne Theory	^{21}Ne Exp.	^{21}Na Theory	^{21}Na Exp.
$\frac{5}{2}^+ \to \frac{3}{2}^+$	$B(M1)$	0.084	0.072 ± 0.001 [b]	0.110	0.083 ± 0.001 [c]
	$B(E2)$	28	24 ± 3 [b]	32	36 ± 20 [c]
	$x(E2/M1)$	+0.074	+0.074 ± 0.005 [b]	−0.065	−0.08 ± 0.03 [d]
	τ (ps)	8.7	10.18 ± 0.16 [b]	7.8	10.42 ± 0.12 [e]
$\frac{1}{2}^+ \to \frac{3}{2}^+$	$B(M1)$	0.27	•••	0.34	0.80 ± 0.22 [f]
	$B(E2)$	1.3	•••	2.5	•••
	$x(E2/M1)$	−0.071	•••	+0.075	•••
	τ (fs)	5.3	≤20 [d]	6.5	2.8 ± 0.8 [g]
$\frac{1}{2}^+ \to \frac{5}{2}^+$	$B(E2)$	0.74	•••	0.85	< 20 ± 6 [h]
	τ (ps)	3.7	•••	6.9	> 0.14 ± 0.04 [h]
$\frac{1}{2}^- \to \frac{1}{2}^+$	$B(E1)$	9.5×10^{-5}	•••	9.5×10^{-5}	$(2.3 \pm 0.5)\times10^{-3}$ [h]
	τ (ps)	•••	•••	3×10^{3}	11 ± 2 [h]
$\frac{1}{2}^- \to \frac{5}{2}^+$	$B(M2)$	0.37	0.48 ± 0.02 [c]	0.26	≤1.2 ± 0.4 [h]
	$B(E3)$	8.0	12 ± 5 [c]	9.3	$\leq(2.2 \pm 0.7)\times10^{3}$ [h]
	$x(E3/M2)$	−0.11	−0.12 ± 0.03 [b]	+0.14	•••
	τ (ps)	184	141 ± 8 [i]	243	54 ± 22 [h]
$\frac{1}{2}^- \to \frac{3}{2}^+$	$B(E1)$	7.1×10^{-5}	$\leq(8.5\pm0.5)\times10^{-8}$ [c]	7.1×10^{-5}	$\leq(3.2 \pm 0.8)\times10^{-6}$ [h]
	$B(M2)$	8.5×10^{-4}	≤ 0.050 ± 0.003 [c]	0.19	≤1.9 ± 0.4 [h]
	$\lvert x(M2/E1)\rvert$	0.13 [j]	•••	0.33 [j]	•••
	τ (ps)	•••	696 ± 50 [i]	•••	18 ± 4 [h]

[a] The transition strengths, $B(EL)$ and $B(ML)$, are in Weisskopf units (Ref. 11), the mixing ratios $x(L+1/L)$ are dimensionless, and the units for the mean lifetimes, τ, are given.

[b] See text.

[c] Calculated from τ and the mixing ratio.

[d] Reference 10.

[e] Reference 15.

[f] Assuming negligible contribution from the $E2$ component, a 100% branch (see Ref. 10), and the listed mean life.

[g] Unweighed average of 2.1 ± 0.5 fs (Ref. 15) and 3.9 ± 1.1 fs[A. Anttila, J. Keinonen, and M. Bister, J. Phys. G 3, 1241 (1977)].

[h] C. Rolfs, W. S. Rodney, M. H. Shapiro, and H. Winkler, Nucl. Phys. A241, 460 (1975).

[i] From the branching ratios of Ref. 22, and the mean life $\tau = 117 \pm 5$ ps (Fig. 1) which is the weighed average of 110 ± 10 ps [D. Schwalm, Ph. D. dissertation, University of Heidelberg, 1969 (unpublished)] and 123 ± 10 ps (Ref. 22). An earlier value of 84 ± 10 ps [Ref. 35] for this mean life is retracted by the authors since the variation of the ^{4}He(^{18}O,n)^{21}Ne cross section with ^{18}O energy was not considered and produces sufficient uncertainty to negate the measurements.

[j] Obtained from the experimental lifetime, τ_{exp}, and the theoretical $M2$ lifetime, τ_{M2}, i.e., $x(M2/E1) = r/(1-r)$ where $\tau_{exp}/\tau_{M2} = r$.

radial matrix elements. Bare nucleon g factors are used for $M1$ and $M2$ transitions. For $E2$ and $E3$ transitions we use effective charges of $1.5e$ and $0.5e$ for protons and neutrons, respectively; for $E2$ transitions this is standard practice and for $E3$ transitions these effective charges give good agreement for the strong $3_1^- \to$ g.s. transitions observed in ^{16}O and ^{20}Ne. The bare charge is used for the $E1$ operator, i.e., an isovector charge of $e/2$. The isoscalar $E1$ matrix element should be zero and this provides a useful check on our wave functions. We also take into account contributions from the spin dependent part of the $E1$ operator [Q'_{LM} defined in Eq. (3.17) of Rose and Brink[13]].

The experimentally measured electromagnetic matrix elements for the transitions of interest are collected in Table II where they are compared with the results of the large basis calculation. Since the properties of the mirror nucleus are useful in helping to evaluate the success of the shell-model description we include the data on ^{21}Na also.

In addition it is necessary to examine the effect of the size of $\frac{1}{2}^-$ basis on the values of the electromagnetic matrix elements. The results of the small and large basis calculations are given in Table III. In the case of the large basis calculation we give a range of values. These represent the results from four calculations; one includes only those (53) configurations with orbital angular momentum $L = 1$, one includes all (53) configurations, and for both these cases two different separations between the sd and pf shells. Since the $\frac{1}{2}^+$ wave function is predominantly $L = 0$, $L = 1$ configurations in the $\frac{1}{2}^-$ wave function should make the most important contributions to the parity-

TABLE III. Effect on the electromagnetic matrix elements of varying the shell–model basis.

Transition	Quantity	^{21}Ne Small	^{21}Ne Large	^{21}Na Small	^{21}Na Large
$\frac{1}{2}^- \rightarrow \frac{5}{2}^+$	$B(M2)$	0.28	0.36 → 0.39	0.10	0.24 → 0.29
	$B(E3)$	5.4	7.8 → 8.0	5.7	9.1 → 9.3
	$x(M2/E3)$	−0.10	−(0.10 → 0.11)	0.17	0.13 → 0.14
$\frac{1}{2}^- \rightarrow \frac{3}{2}^+$	$B(E1)$	1.5×10^{-4}	$(3.0 \rightarrow 7.1) \times 10^{-5}$	Same as ^{21}Ne	
	$B(M2)$	1.6×10^{-2}	$(1.6 \rightarrow 8.5) \times 10^{-4}$	0.17	0.19 → 0.22
	$\lvert x(M2/E1) \rvert$	0.67	0.06 → 0.13	0.31	0.33 → 0.36
$\frac{1}{2}^- \rightarrow \frac{1}{2}^+$	$B(E1)$	9.5×10^{-5}	$(2.7 \rightarrow 9.5) \times 10^{-5}$	Same as ^{21}Ne	

mixing matrix element. Also since the $\frac{1}{2}^-_2$ wave function is dominated by a single $(sd)^4(pf)$ configuration, expanding the basis tends to push down the $\frac{1}{2}^-_1$ level more than the $\frac{1}{2}^-_2$ level. Therefore if we wish to maintain the separation between the two $\frac{1}{2}^-$ levels we must reduce the single particle energies for the pf orbits by about 700 keV. Even such a small change can have a significant effect on the weaker $E1$ and $M2$ matrix elements.

The description of transitions between the positive parity levels is quite satisfactory especially for the in-band $\frac{5}{2}^+ \rightarrow \frac{3}{2}^+$ transition. A new measurement of the lifetime of the $\frac{1}{2}^+$ level in ^{21}Ne needs to be made to determine experimentally the $M1$ matrix element which appears in the expression for ϵ_1 [see Eq. (17)].

The calculated $B(M2)$ for the $\frac{1}{2}^- \rightarrow \frac{5}{2}^+$ transition in ^{21}Ne agrees well with the measured value but the factor of 4 disagreement in ^{21}Na is disturbing. The calculated mixing ratio for the same transition also agrees very well with the present measurement.

Although we cannot hope to reproduce the observed $E1$ matrix element for the $\frac{1}{2}^- \rightarrow \frac{3}{2}^+$ transition we do predict a very small $B(E1)$ of 7×10^{-5} W.u. It is interesting to note that the spin part of the $E1$ operator gives by itself a matrix element which is as large as the observed matrix element; in this case there is an isoscalar contribution which can lead to a difference in the $B(E1)$ values for ^{21}Ne and ^{21}Na. The contribution from the spin part of the $E1$ operator has not been considered in previous attempts to explain the small $E1$ matrix element. At this level relativistic corrections should also be considered. We have checked that higher order terms in the expansion of $j_1(kr)$ are not important. The effects of isospin mixing could be important since typical isospin forbidden $E1$ strengths in ^{18}F and ^{20}Ne are of the order of 10^{-5} W.u. The $B(E1)$ values that we quote in Tables II and III are those for the normal $E1$ operator alone.

The $B(M2)$ for the $\frac{1}{2}^- \rightarrow \frac{3}{2}^+$ transitions in ^{21}Ne is predicted to be small, the result of a cancellation between the isoscalar and isovector matrix elements. The details of this cancellation are shown in Table IV. It may be seen that the orbital isovector and spin isoscalar matrix elements are small in both calculations and that the cancellation occurs between the orbital isoscalar and spin isovector matrix elements which are both moderately large considering the intrinsic inhibition of this transition.[35] In ^{21}Na the $B(M2)$ is much larger implying that the branching ratios for the decay of the $\frac{1}{2}^-$ level to the $\frac{5}{2}^+$ and $\frac{3}{2}^+$ levels should be very different in the two nuclei as is indeed observed.

For the important $M2/E1$ mixing ratio of the $\frac{1}{2}^- \rightarrow \frac{3}{2}^+$ transition in ^{21}Ne we can only make an estimate based on the measured partial γ width and the calculated $M2$ width. This gives $\lvert x_3 \rvert = 0.13$. Since both the $B(E1)$ and the $B(M2)$ are small the mixing ratio is a very difficult quantity to estimate theoretically and no estimate can be made of the sign. Thus the difficult experiment to measure this quantity must be attempted.

The $B(E1)$ for the $\frac{1}{2}^- \rightarrow \frac{1}{2}^+$ transition is predicted to be quite small in disagreement with the strength observed in ^{21}Na. The fact that the $\frac{1}{2}^+$ level in ^{21}Na is unbound and exhibits a large level shift adds an additional theoretical difficulty.

E. Circular polarization and asymmetry

Using the theoretical results presented in Table II together with the experimental values of ΔE and the partial half-life of the $\frac{1}{2}^- \rightarrow \frac{3}{2}^+$ transition we can make an estimate for $\lvert A_\gamma \rvert$ or $\lvert P_\gamma' \rvert$, as defined in

TABLE IV. Details of the cancellation in the $M2$ $\frac{1}{2}^- \rightarrow \frac{3}{2}^+$ matrix element.

Matrix element	Small basis	Large basis
$\langle r[Y^1,l]^2 \rangle$	−1.009	−0.857
$\langle r[Y^1,l]^2\tau \rangle$	−0.006	−0.037
$\langle r[Y^1,s]^2 \rangle$	−0.058	−0.058
$\langle r[Y^1,s]^2\tau \rangle$	0.579	0.836
Total	−0.494	−0.116

Eqs. (14) and (12), respectively, in terms of the parity-mixing matrix element. We have

$$|A_\gamma| = |KP_W(\tfrac{1}{2})\langle \tfrac{1}{2}^+ | V_{\rm PNC} | \tfrac{1}{2}^- \rangle| \quad (20a)$$

with

$$K = [\tau(E1)/\tau(M1)]^{1/2} f_1'(\tfrac{1}{2}, \tfrac{3}{2})/\Delta E\,, \quad (20b)$$

where $\tau(M1)$ and $\tau(E1)$ are the partial dipole half-lives for the ground-state decays of the $\frac{1}{2}^+$ and $\frac{1}{2}^-$ states, respectively. Inserting the experimental and theoretical values of Table II for $\tau(E1)$ and $\tau(M1)$, respectively, we find $K = 6.3 \times 10^4$ MeV^{-1} for $x_3 = -0.13$ and $K = 4.2 \times 10^4$ MeV^{-1} for $x_3 = +0.13$. Also

$$|P_\gamma'| = |L\langle \tfrac{1}{2}^+ | V_{\rm PNC} | \tfrac{1}{2}^- \rangle|\,, \quad (20c)$$

where

$$L = 2[\tau(E1)/\tau(M1)]^{1/2} f_0'(\tfrac{1}{2}, \tfrac{3}{2})/\Delta E \quad (20d)$$

and we find $L = 9.4 \times 10^4$ MeV^{-1} essentially independent of the sign of x_3 (we have taken the average of the values for $x_3 = \pm 0.13$). The aim of the experiments on the electromagnetic properties of the ^{21}Ne levels is, for present purposes, an experimental determination of K and L.

The value obtained for K from the calculations is large compared with the corresponding value of 2×10^2 MeV^{-1} for ^{19}F. Thus, unless the parity mixing matrix element is very small, a measurement of the asymmetry or the circular polarization of the $\frac{1}{2}^- \to \frac{3}{2}^+$ transition should be feasible. A calculation of the parity-mixing matrix element using the two body PNC interaction is beyond the scope of our existing shell model code. Instead we use the effective one body PNC interaction

$$V_{\rm PNC} = -\vec{\sigma} \cdot \vec{p}[1 \pm 0.3\tau_3] \times 10^{-6}\,, \quad (21)$$

where the strength constants of the isoscalar and isovector terms are taken from the study by Box, Gabric, and McKellar[36] of parity mixing in ^{19}F and are appropriate for the Cabibbo model of weak interactions. Then for the magnitude of the circular polarization we obtain $(0.42 \pm 0.06)\%$ from the small basis calculation where the two terms represent the isoscalar and isovector contributions, respectively. From the large basis calculation we obtain values in the range $(1.09 \to 1.19)\%$ and $(0.16 \to 0.17)\%$ for the two terms. We note that although the circular polarization is sensitive to the basis size it may be classed with the $E3$ and the stronger $M2$ transitions displayed in Table III in the sense that its sensitivity to variations in the large basis calculation is quite small. A choice of sign for the contribution of the isovector term in Eq. (21) may be made to reproduce the observed asymmetry in ^{19}F which is negative.[7] This choice gives for the parity-mixing observables in ^{18}F (Ref. 9), ^{19}F (Ref. 6), and ^{21}Ne (using our wave functions in all cases):

$$^{18}\text{F:}\quad |P_\gamma'| = 3.4 \times 10^{-4}\,, \quad (22a)$$

$$^{19}\text{F:}\quad \delta = A_\gamma/P_W(\tfrac{1}{2}) = (4.2 - 1.1) \times 10^{-5}\,, \quad (22b)$$

$$^{21}\text{Ne:}\quad |P_\gamma'| = (1.19 + 0.17) \times 10^{-2}\,. \quad (22c)$$

In addition to the choice of sign, Eq. (22b) shows that an enhancement of the isovector term is necessary to make δ negative. This is in agreement with predictions from some weak interaction models which include neutral currents (see Ref. 6). The same enhancement would then predict a $(2 \to 3)\%$ circular polarization in ^{21}Ne. This value for the circular polarization is larger than the limit of $(0.1 \pm 0.5)\%$ obtained in a recent experiment.[37]

The relative sign of the isovector contributions in ^{19}F and ^{21}Ne may be easily understood on the basis of a simple model for the wave functions. If the $\frac{1}{2}^-$ wave functions in ^{19}F and ^{21}Ne are of the form $p^{-1}(sd)^4(T=0)$ (which is a good approximation) and $p^{-1}(sd)^6(T=1)$ (~80% in our calculation) respectively, then, for any one body operator connecting the hole states to $(sd)^n$ configurations, the ratios of the isovector to the isoscalar matrix elements in the two nuclei are related by[35]

$$\frac{v}{s}(^{19}\text{F}) = -3\,\frac{v}{s}(^{21}\text{Ne})\,. \quad (23)$$

In the special case of the operator $\vec{\sigma} \cdot \vec{p}$ the full shell model wave functions gives -1.73 instead of the -3 of Eq. (23) from the simple model.

V. DISCUSSION

In contrast to the situation in ^{19}F the electromagnetic matrix elements needed to extract a parity-mixing matrix element from a measured circular polarization or asymmetry in ^{21}Ne are not well known. In fact, of the two lifetimes and two mixing ratios which must in principle be measured, only the lifetime of the $\frac{1}{2}^-$ level has been measured.[38] Accordingly our emphasis in this paper has been on the electromagnetic properties of levels involved in possible parity-mixing experiments in ^{21}Ne.

In practice we do not need to know accurately the $E2/M1$ mixing ratio for the $\frac{1}{2}^+ \to \frac{3}{2}^+$ transition since it is intrinsically small. We can therefore use the value calculated from theory. Thus two measurements remain to be made.

(1) Lifetime of the $\frac{1}{2}^+$ level. The predicted lifetime of 5 fs is close to the limit for a Doppler-shift-attenuation measurement and it will be difficult to measure the lifetime with high precision.[38] An alternative would be to use the fact that the calculated matrix element is mainly isovector to relate the lifetime in ^{21}Ne to that in ^{21}Na. Unfortun-

ately neither the two experimental measurements in ^{21}Na nor the calculated value are in particularly good agreement with each other. Alternatively, one could probably rely on the theoretical value for this strong $M1$ matrix element with an accuracy of ~±20%.

(2) $M2/E1$ mixing ratio for the $\frac{1}{2}^- \rightarrow \frac{3}{2}^+$ transition. The measurement of the $E3/M2$ mixing ratio described in Sec. III represents the first step towards obtaining the $M2/E1$ mixing ratio. The experiment, suggested in Sec. II, to measure the $M2/E1$ mixing ratio in terms of the $E3/M2$ mixing ratio is an extremely difficult one. However, it is the only means available to help determine the sign of the parity-mixing matrix element which it is important to know in order to most fully test different weak interaction models. In addition, if the parity mixing is very small, the only possible measurement may be an asymmetry measurement (if a reasonable polarization transfer reaction can be found) in which case this mixing ratio is necessary for a quantitative interpretation of such a result.

Our shell-model calculations give quite good agreement with the electromagnetic data available on ^{21}Ne. Some of the weaker $E1$ and $M2$ matrix elements are very sensitive to the precise details of the calculation. The $M2$ matrix element on which the important mixing ratio x_3 depends is in this class of matrix elements. The parity-mixing matrix element, on the other hand, is relatively speaking much larger and displays less sensitivity to the finer details of the calculation. This is true for the individual isoscalar and isovector contributions and should hold for the full matrix element provided that the relative sign of the isoscalar and isovector contributions is indeed positive. The most important improvement to be made in the calculation of the parity-mixing matrix element is to perform it using the two body PNC interaction. Clearly, it is also desirable to study the sensitivity of the parity-mixing matrix element to further increases in basis size and to variations in the effective interactions and single particle energies. For example, there is a 12% component of (24) symmetry in the $\frac{1}{2}^+$ wave function (see Table I) which suggests that configurations with (34), (15), and (23) symmetry should be added to the $\frac{1}{2}^-$ basis (at least in perturbation theory). Also, in this paper our attention has been directed towards small components in the $\frac{1}{2}^-$ wave function which can connect via the $\vec{\sigma}\cdot\vec{p}$ operator to the dominant $0\hbar\omega$ components of the $\frac{1}{2}^+$ wave function; we should also consider on the same footing small $2\hbar\omega$ components in the $\frac{1}{2}^+$ wave function which can connect via the same operator to the dominant $1\hbar\omega$ configurations in the $\frac{1}{2}^-$ wave function.

We note that the $\vec{\sigma}\cdot\vec{p}$ operator, and presumably the more fundamental two-body PNC interaction, may be classed with the $E1$ and $M2$ operator, which also depend on a single coordinate or momentum. Its largest matrix elements will, therefore, not in general be between two low-lying states. This limits the precision with which we can hope to calculate parity-mixing matrix elements. However, the parity-mixing matrix elements in ^{18}F, ^{19}F, and ^{21}Ne appear large enough that the reliability of the calculation should be comparable to that for the stronger $M2$ matrix elements.

ACKNOWLEDGMENTS

This research was supported by the Division of Basic Energy Sciences, Department of Energy. The experimental part of this work was done while E.K.W. was a visitor of the University of Washington.

[1]D. H. Wilkinson, Phys. Rev. 109, 1603 (1958); N. Tanner, *ibid.* 107, 1203 (1957).
[2]T. D. Lee and C. N. Yang, Phys. Rev. 104, 254 (1956).
[3]C. S. Wu, E. Ambler, R. W. Hayward, D. D. Hopper, and R. P. Hudson, Phys. Rev. 105, 1413 (1957).
[4]N. Neubeck, H. Schober, and H. Wäffler, Phys. Rev. C 10, 320 (1974).
[5]M. Gari, Phys. Rep. 6C, 319 (1973).
[6]E. G. Adelberger, in Proceedings of the Ben Lee Memorial International Conference on Parity Nonconservation, Weak Neutral Currents and Gauge Theories, 1977, Fermi National Accelerator Laboratory (unpublished).
[7]E. G. Adelberger, H. E. Swanson, M. D. Cooper, J. W. Tape, and T. A. Trainor, Phys. Rev. Lett. 34, 402 (1975).
[8]See Ref. 6, for a discussion of this point and a list of references.
[9]C. A. Barnes, M. M. Lowry, J. M. Davidson, R. E. Marrs, F. B. Moringo, B. Chang, E. G. Adelberger, and H. E. Swanson, Phys. Rev. Lett. 40, 840 (1978).
[10]P. M. Endt and C. van der Leun, Nucl. Phys. A214, 1 (1973); Nucl. Phys. (to be published).
[11]For a definition of the Weisskopf unit see S. J. Skorka, J. Hertel, and T. W. Retz-Schmidt, Nucl. Data A2, 347 (1966).
[12]B. H. J. McKellar, Contribution to the Third Vacation School of the Australian Institute of Physics, Jindabyne, New South Wales, 1977 (unpublished).
[13]H. J. Rose and D. M. Brink, Rev. Mod. Phys. 39, 306 (1967).
[14]D. Schwalm, E. K. Warburton, and J. W. Olness,

Nucl. Phys. A293, 425 (1977).
[15]H. L. Berg, W. Hietzke, C. Rolfs, and H. Winkler, Nucl. Phys. A276, 168 (1977).
[16]P. M. Rowe, J. Asher, H. A. Doubt, M. A. Grace, P. D. Johnston, and T. J. Moorhouse, J. Phys. G (London) 4, 431 (1978).
[17]F. A. Beck, T. Byrski, G. J. Costa, and J. P. Vivien, Phys. Rev. C 16, 679 (1977).
[18]E. K. Warburton and J. W. Olness, Phys. Rev. C 2, 2235 (1970).
[19]J. G. Pronko, W. C. Olsen, and J. T. Sample, Nucl. Phys. 83, 321 (1966).
[20]K. A. Snover, R. von Lintig, P. G. Ikossi, and E. K. Warburton, Bull. Am. Phys. Soc. 23, 520 (1978).
[21]P. M. Endt and C. van der Leun, At. Data Nucl. Data Tables 13, 67 (1974); Nucl. Phys. A235, 27 (1974).
[22]R. M. Freeman, F. Haas, B. Heusch, and A. Gallmann, Nucl. Phys. A261, 471 (1976).
[23]T. T. S. Kuo and G. E. Brown, Nucl. Phys. 85, 40 (1966).
[24]T. T. S. Kuo, Nucl. Phys. A103, 71 (1967).
[25]B. M. Preedom and B. H. Wildenthal, Phys. Rev. C 6, 1633 (1972).
[26]W. Chung, Ph.D. thesis, Michigan State University, 1976 (unpublished).
[27]C. Rolfs, E. Kuhlmann, F. Riess, and R. Kraemer, Nucl. Phys. A167, 449 (1971).
[28]B. E. Chi, Nucl. Phys. 83, 97 (1966).
[29]J. P. Draayer, Nucl. Phys. A237, 157 (1975).
[30]C. Rolfs, H. P. Traut-vetter, E. Kuhlmann, and F. Riess, Nucl. Phys. A189, 641 (1972).
[31]A. J. Howard, J. G. Pronko, and C. A. Whitten, Nucl. Phys. A152, 317 (1970).
[32]E. C. Halbert, J. B. McGrory, B. H. Wildenthal, and S. P. Pandya, *Advances in Nuclear Physics*, edited by M. Baranger and E. Vogt (Plenum, New York, 1971), Vol. 4.
[33]D. J. Millener (unpublished).
[34]D. J. Millener and D. Kurath, Nucl. Phys. A255, 315 (1975).
[35]E. K. Warburton, J. W. Olness, G. A. P. Engelbertink, and K. W. Jones, Phys. Rev. C 3, 2344 (1971).
[36]M. A. Box, A. J. Gabric, and B. H. J. McKellar, Nucl. Phys. A271, 412 (1976).
[37]K. A. Snover, R. von Lintig, E. G. Adelberger, H. E. Swanson, T. A. Trainor, A. B. McDonald, E. D. Earle, and C. A. Barnes, Phys. Rev. Lett. 41, 145 (1978).
[38]Actually, a published value of $\tau = 10 \pm 4$ fs for the mean life of the $\frac{1}{2}^+$ level does exist [H. Grawe, F. Heidinger, and K. Kändler, Z. Phys. A280, 271 (1977)]. However, the accuracy of this measurement is not really adequate for present purposes.